Event-Triggered Data-Driven Control for Nonlinear Systems Under Frequency-Duration-Constrained DoS Attacks

Xuhui Bu, *Member, IEEE*, Wei Yu, *Student Member, IEEE*, Yanling Yin, and Zhongsheng Hou, *Fellow, IEEE*

***Abstract*— This paper addresses the event-triggered model free adaptive control (MFAC) problem for unknown nonlinear systems under denial-of-service (DoS) attacks, where the design and analysis are discussed under the data-driven framework. Firstly, by using the novel pseudo partial derivative, the nonlinear systems are converted into an equivalent data-relationship model. Then, the DoS attacks are described as limited by their frequency and duration, and without any more specific assumptions about the attack structure or strategy. Next, a novel event-triggered MFAC scheme is proposed. By employing the Lyapunov stability theory, the stability performance is analyzed. Furthermore, a compensation algorithm is designed to against the adverse impact brought by the DoS attacks. Finally, simulations including a numerical example and a load frequency control (LFC) example for multi-area power systems are given to demonstrate the validity and applicability of the proposed schemes.**

***Index Terms*— Event-triggered control, DoS attacks, unknown nonlinear systems, model free adaptive control, data-driven design.**

I. Introduction

IN RECENT years, due to the rapid development and cross integration of computer science and communication technology, the framework of cyber physical systems (CPSs) has been widely and effectively applied in various industrial fields [1], [2], [3]. CPSs possess the ability to improve the collaboration efficiency of network physical elements and enhance system intelligence. These capabilities are driving a wide range of applications of CPSs in infrastructure, wearable devices, transportation systems, smart grids, etc [4], [5], [6], [7]. It is important to take the potential network-induced phenomena into consideration when analyzing the controller, including malicious networked attacks that will affect the availability and integrity of the system.

Actually, two types of attack models are generally considered when the security control issue of CPSs is discussed, namely deception attacks and denial-of-service (DoS) attacks. The former attempts to destroy the integrality of the controller and actuator data by injecting false signals via the transmission networks, such as replay attacks and false injection attacks [8], [9], [10]. Moreover, the latter aims at interfering the transmission channels to obstruct the transmission of system data [11], [12]. Recently, some results have been published in the control field of CPSs under DoS attacks. In [13] and [14], a novel framework of DoS attacks is introduced for the first time. This attack framework only restricts the frequency and duration of the attacks, and does not make any specific assumptions about the structure of the attack strategy. In [15], a switched state estimator is established by employing the average dwell time method and combining the duration and frequency of the jamming attacks. The influence brought by DoS attacks is studied in [16] while investigating the resilient filtering problem for power systems. The communication structure which can prevent malicious DoS attacks from destroying system stability is studied in [17]. Meanwhile, the game between attackers and defenders has also provoked widespread discussion. In [18], the game theory is studied under a Stackelberg game viewpoint of UAV-aided traffic monitoring network. In [19], the Stackelberg Equilibrium approach is used to analyze the game strategies. In addition, the defense strategy is rather important for the security operation of practical systems. In [20], the smart transmission power level is selected with the combination of the defensive deception to against jamming attacks.

It is worth noting that the introduction of transmission network in CPSs also raises concerns about the potential issues caused by bandwidth constraints. Fortunately, compared with the fixed time-triggered mechanism based on periodically sampling, the event-triggered mechanism based on flexible triggering conditions is widely considered to be a feasible solution to such difficulties [21], [22], [23]. The research of event-triggered control has been reported in plenty of literature. For example, the event-triggered active disturbance rejection

Manuscript received 22 August 2022; revised 13 November 2022; accepted 14 December 2022. Date of publication 29 December 2022; date of current version 9 February 2023. This work was supported in part by the National Natural Science Foundation of China under Grant U1804147, Grant 62273133, Grant 61833001, and Grant 62203151; in part by the Innovative Scientists and Technicians Team of Henan Polytechnic University under Grant T2019-2; and in part by the Innovative Scientists and Technicians Team of Henan Provincial High Education under Grant 20IRTSTHN019. The associate editor coordinating the review of this manuscript and approving it for publication was Prof. Mika Ylianttila. *(Corresponding author: Yanling Yin.)*

Xuhui Bu and Wei Yu are with the School of Electrical Engineering and Automation, Henan Polytechnic University, Jiaozuo 454003, China (e-mail: buxuhui@gmail.com; yuwei5150@163.com).

Yanling Yin is with the Research Center for Energy Economics, School of Business Administration, Henan Polytechnic University, Jiaozuo 454003, China (e-mail: yyl1981hpu@126.com).

Zhongsheng Hou is with the School of Automation, Qingdao University, Qingdao 266071, China (e-mail: zhshhou@bjtu.edu.cn).

Digital Object Identifier 10.1109/TIFS.2022.3233154

control scheme is established in [24] with an extended state observer for disturbed systems. In [25], the observer-based control problem with event-triggered mechanism is studied, and both the continuous and discrete-time event detectors are designed. In [26], the global stabilization issues for the general linear systems via event-based bounded control are studied. In addition, some results have been also obtained in the design of event-triggered mechanism for nonlinear systems. For instance, the event-triggered control issue is studied in [27] and [28] while designing the sliding mode controller for the systems with nonlinear and uncertain dynamics. In [29], the model predictive control problem for nonlinear systems is considered with event-triggered mechanism. In [30], the nonlinear nonholonomic robot is controlled with the event-based model predictive tracking control method. Nonetheless, the results in [27], [28], [29], and [30] all require that the system structure be known or at least partially known, which is usually a harsh condition. In addition, the existing robust event-triggered control approaches for nonlinear systems are still dependent on model information, which brings challenges to their practical application [31], [32].

Although considerable results have been achieved in the study of event-triggered control, the security-related data-driven event-triggered research of CPSs is still rare. Some pioneer results in this field have been reported. In [33], an event-triggered resilient control is stated for those systems subject to periodic DoS jamming attacks, where the relationship between triggering and DoS parameters is characterized quantitatively. In [34], the consensus tracking issue for the multi-agent systems is investigated with a design of event-triggered mechanism to against DoS attacks. Meanwhile, almost all practical systems contain complex nonlinearities, and the accurate dynamic model is rather difficult to acquire. How to analyze and construct the event-triggered control schemes for these unknown nonlinear systems under the network attacks is still an urgent issue to be addressed. The main difficulties are as follows.

1) How to design the data-driven control scheme for the nonlinear systems subject to unknown dynamics and malicious attacks?

2) How to establish the triggering condition that balance both stability performance and bandwidth occupancy?

3) How can the controller be improved to against the frequency-duration-constrained DoS attacks?

Fortunately, model free adaptive control (MFAC) is an effective method for systems with unknown and nonlinear dynamics [35], [36], [37]. A new dynamic linearization technique is introduced in this method such that the linear data-relationship model of the nonlinear systems can be established. On this basis, a data-driven control scheme is constructed only depending on the input and output (I/O) information, and the stability analysis is also given without using any model information. Due to the data-driven merit, MFAC has been successfully applied to a variety of practical processes, such as [38], [39], [40], [41], and [42]. Nevertheless, the effect of network attacks on system stability and how to design event-triggered control scheme under the data-driven framework have not been explored yet. Therefore, the main work of the paper is to contribute to the event-triggered MFAC issue for unknown nonlinear systems under DoS attacks. By comparing with the existing researches, the main contributions are summarized as:

1) Compared with [13], [14], [15], [16], [17], [18], [19], [20], [21], [22], [23], [24], [25], [26], [27], [28], and [29], this is the first time that the security control and the event-triggered mechanism are studied under the unified data-driven framework, where the controller and the triggering conditions are completely independent to model information.

2) In contrast to the contractive mapping principle in [35], [36], [37], [38], [39], [40], [41], and [42], the system stability is analyzed by employing the Lyapunov approach combined with the event-triggered conditions in this paper, which expands the theoretical tools of MFAC.

3) The compensation scheme is designed by assigning estimation capabilities to the proposed controller, which can against the potential adverse effect brought by the malicious DoS attackers.

The rest of the paper is formulated as: The system description, the introduction of DoS attacks and event-triggered mechanism are provided in Section II. The convergence analysis of the proposed algorithm is introduced in Section III. Section IV illustrates the analysis and design of the proposed compensation algorithm. The simulation results are given in Section V and conclusions of this paper are stated in Section VI.

Notation: Let $\mathbb{R}^l$ denote the set of $l-$dimensional real vector space, and $\mathbb{Z}^+$ denote the set of positive integers. Denote $round\,(\delta)$ by the function that rounds δ to the nearest integer. Let Δ denote the difference between the two adjacent time instants of the variable. The usual Euclidean vector norm is represented by $|\cdot|$. Denote a^{-1} as the reciprocal of a, and i is the number of attacks. A function $\partial(\cdot):[0,\infty)\to\mathbb{R}$ is said to be of class K_∞ function if it satisfies: strictly increasing, $\partial(0)=0$ and $\partial(s)\to\infty$ as $s\to\infty$.

II. Problem Formulation

A. System Descriptions

A class of discrete-time single-input single-output (SISO) nonlinear systems is considered as follows.

$$y(k+1)=f(y(k),u(k)) \tag{1}$$

where $k\in\mathbb{Z}^+$, $y(k)\in\mathbb{R}^1$, $u(k)\in\mathbb{R}^1$ and $f(\cdot):\mathbb{R}\mapsto\mathbb{R}^1$ denote the time instant, system output, control input and an unknown nonlinear function respectively.

Remark 1: The nonlinear systems (1) represent a class of typical SISO non-affine systems, which have two main characteristics: 1) Nonlinearity, which is reflected in the function $f(\cdot)$; 2) Unknown feature, which mainly means that the specific mapping relationship is unknown to the controller designer. Therefore, such form can represent a large class of practical applications including temperature control system, pressure control system, etc.

The following two assumptions are given for further discussion.

Assumption 1: The partial derivative of nonlinear function $f(\cdot)$ with respect to $u(k)$ is continuous.

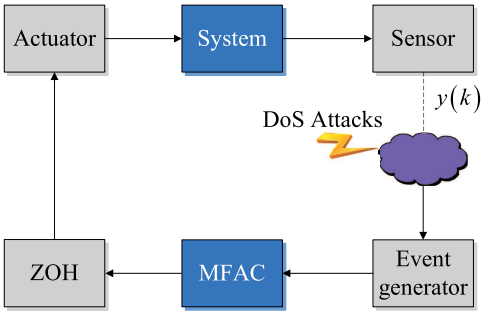

Fig. 1. Structure of the event-triggered CPSs under DoS attacks.

Assumption 2: The system (1) satisfies the generalized Lipschitz condition, that is, if $\Delta u(k) \neq 0$, then $|\Delta y(k+1)| \leq b|\Delta u(k)|$ holds for any k, where $\Delta y(k+1) = y(k+1) - y(k)$, $\Delta u(k) = u(k) - u(k-1)$, and b denotes a positive constant.

Remark 2: Assumption 1 is a constraint condition in controller design for practical nonlinear systems, which has been discussed in [35], [36], and [37]. This condition is usually a necessary assumption in other model-based control approaches. In addition, the change of the system output can be effectively limited by Assumption 2. For the energy expenditure, the change of the output energy, which is produced by bounded input energy, should also be bounded, such as welding system, and motor control system, etc. Therefore, Assumptions 1-2 are both reasonable and acceptable for the practical applications.

Lemma 1: For the nonlinear systems (1) satisfying Assumptions 1-2, if $\Delta u(k) \neq 0$, then there exists a parameter $\phi(k) \in \mathbb{R}^1$, which is called pseudo partial derivative (PPD), such that the system can be converted into a compact form dynamical linearization (CFDL) model

$$\Delta y(k+1) = \phi(k)\Delta u(k) \tag{2}$$

where $|\phi(k)| \leq \bar{b}$ for any k, and $\bar{b}$ is a positive constant.

Proof: The detailed derivation can refer to [35], [36], and [37]. ■

Thus, $\phi(k)$ is only related to the I/O data of the system up to the sampling instant k, and does not contain or imply the structure and parameter information of the dynamic model (1). The linear model (2) is a data model that is equivalent to the original nonlinear model only for controller design.

Remark 3: It is worth noting that the parameter $\phi(k)$ is a concept in a mathematical sense, whose existence is only theoretically guaranteed by rigorous proof. All possible complex behavior characteristics of the nonlinear systems (1), such as nonlinearity, time-varying parameters or structures, are compressed into the time-varying scalar parameter $\phi(k)$. Nevertheless, the dynamic characteristics of $\phi(k)$ may be too complex to describe mathematically in detail, but its numerical behavior may be relatively simple and easy to estimate.

The event-triggered MFAC mechanism is implemented in a networked environment and the structure is shown in Fig. 1. It is assumed that the system output $y(k)$ is subject to intermittent DoS attacks during transmissions, which will prevent the event generator from receiving the latest output. The event generator is applied to determine the signal sequence transmitted to the MFAC, and the zero-order holder (ZOH) is designed to hold the control input when the MFAC does not receive the latest output. The modeling of the intermittent DoS attacks and the event-triggered mechanism are described in detail below.

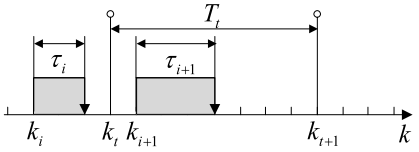

Fig. 2. Attack sequence and triggering instants.

B. Intermittent DoS Attacks

Consider a type of intermittent DoS attacks shown in Fig. 2. Noting that although the attack strategy of external attacker is unknown and unpredictable, its attack results can be detected by employing the on-line detection mechanism. In this paper, we mainly focus on studying the design and analysis issues of the event-triggered MFAC in the existence of DoS attacks, so they are assumed to be always detectable like others work [13], [14].

DoS attack interval means that the attacker maliciously blocks the transmissions among a period of time instants. To be specific, when instant k is within the attack intervals, the system's attempt to transmit $y(k)$ will fail, causing $u(k)$ to fail to update. The i-th attack interval is denoted by

$$K_i = \{k_i\} \cup [k_i, k_i + \tau_i)$$

where K_i determines when the communication is prohibited, and $\{k_i\}_{i\in\mathbb{Z}^+}$ and τ_i denote the set of the transition instants from sleeping to launch of the DoS attacks and the length of i-th attack interval respectively. For any interval $[k_0, k]$, $n(k_0, k)$ represents the transition numbers of DoS status, and the set of DoS interval during $[k_0, k] \subset [0, +\infty)$ is denoted by $\Xi(k_0, k) = \bigcup_{i\in\mathbb{N}_0} K_i \bigcap [k_0, k]$.

In the paper, the attack strategy is assumed to be unknown, and the energy-limited DoS attacks are limited by their frequency and duration. The main assumptions about the DoS attacks are given as follows.

Assumption 3 (DoS Frequency) [13], [43]: For any time interval $[k_0, k] \subset [0, +\infty)$, there exists a positive constant κ_n and a K_∞ function $f_n(k_0, k)$ such that

$$n(k_0, k) \leq \kappa_n + f_n(k_0, k) \tag{3}$$

Assumption 4 (DoS Duration) [13], [43]: For any time interval $[k_0, k] \subset [0, +\infty)$, there exists a positive constant ζ_Ξ and a K_∞ function $f_\Xi(k_0, k)$ such that

$$\Xi(k_0, k) \leq \zeta_\Xi + f_\Xi(k_0, k) \tag{4}$$

The boundary of $|\Xi(k_0, k)|$ means the total length of DoS attacks over time interval (k_0, k). Define $\Theta(k_0, k) := [k_0, k] \setminus \Xi(k_0, k)$ as the length of time intervals during which the attack is inactive, then it yields that

$$\begin{aligned}\Theta(k_0, k) &= k - k_0 - |\Xi(k_0, k)| \\ &\geq k - k_0 - \zeta_\Xi - f_\Xi(k_0, k) - n(k_0, k)\end{aligned} \tag{5}$$

for any $k_0, k \in [0, +\infty)$.

Remark 4: Note that Assumptions 3-4 do not contain any information about the probability distribution of an attacker's strategy, but only indicates the frequency and duration limitations of DoS attacks. Indeed, the attack strategy is mostly not available for the controller designer.

C. Event-Triggered Mechanism Design

Due to the existence of DoS attacks, the triggering scheme is adjusted as: once the attacks are launched, the triggering scheme will stop working for the purpose of saving bandwidth resources. Thus, the next transmission instant $k_{t+1} \in \Theta(k_0, k)$ will be determined by judging the following triggering condition

$$\varpi(k)^2 > 2Q^2(k-1)\Delta y_d^2(k) - \gamma e^2(k-1) \tag{6}$$

where $Q(k) = 1 - \rho\hat{\phi}(k)^2 / \left(\lambda + \left|\hat{\phi}(k)\right|^2\right)$ and $\hat{\phi}(k)$ is the estimation value of $\phi(k)$. The positive constants ρ, λ are adjustable parameters. Moreover, $y_d(k)$ is the desired trajectory and $\Delta y_d(k) = y_d(k) - y_d(k-1)$ denotes its increment. $e(k) = y_d(k) - y(k)$ represents the tracking error and $\varpi(k) = e(k_t) - e(k)$ denotes the triggering error. Noting that $\gamma \in [0, 1]$ is an adjustable triggering parameter to balance the transmission quantity and stability.

The event generator is built in the input side as shown in Fig. 1. The triggering condition is judged at each sampling instant, and the condition (6) holds only if the triggering error $\varpi(k)$ exceeds the threshold. Hence, we define the instant when the inequality (6) is true as the triggering instant k_t, and T_t is the t-th triggering interval. The event-triggered mechanism works as: only when the triggering condition in (6) is satisfied, the latest output sampled from the sensor can be sent to MFAC for updating, otherwise the control signal will remain as the previous value by ZOH. It is worth noting that the lower bound of the inter-execution time $(k+1)T - kT$ is exactly the sampling period $T > 0$, which means the absence of Zeno behavior for discrete-time systems.

The workflow of the event-triggered mechanism is shown in Fig. 3. Firstly, it is determined whether it is under an attack interval for the current time instant before the updating of control input. If it is, update $u(k) = u(k-1)$. If not, the triggering condition will be calculated and judged. Then, if the condition is true, update $u(k)$ with the latest I/O data. If not, update $u(k) = u(k-1)$.

D. Event-Triggered MFAC Algorithm

Construct the criterion function with respect to $u(k)$

$$\mathbf{J}(u(k)) = |e(k+1)|^2 + \lambda|\Delta u(k)|^2$$

where λ represents a positive weighting coefficient. Recalling the linear data model (2) and minimizing the above function, there is

$$u(k) = u(k-1) + \frac{\rho\phi(k)}{\lambda + |\phi(k)|^2}\left(y_d(k+1) - y(k)\right)$$

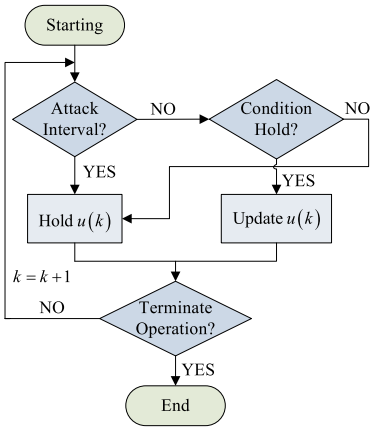

Fig. 3. Workflow diagram of event-triggered mechanism.

where ρ is a step factor added to improve the generality. Next, to estimate the parameter $\phi(k)$, a criterion function is designed

$$\mathbf{J}(\phi(k)) = |\Delta y(k) - \phi(k)\Delta u(k-1)|^2 + \mu\left|\phi(k) - \hat{\phi}(k-1)\right|^2$$

where $\hat{\phi}(k)$ is the estimation value of $\phi(k)$, and $\mu > 0$ is a weighting factor. Next, minimizing above function, one has

$$\hat{\phi}(k) = \hat{\phi}(k-1) + \frac{\eta\Delta u(k-1)}{\mu + |\Delta u(k-1)|^2} \times \left(\Delta y(k) - \hat{\phi}(k-1)\Delta u(k-1)\right)$$

where $\eta \in (0, 1]$ is a step factor.

Seeing that the intermittent DoS attack blocks the transmission channels, $y(k)$ cannot be employed to construct the controller. Therefore, denote

$$z(k) = \begin{cases} y(k), & k = k_t \\ z(k-1), & k \in (k_{t-1}, k_t) \end{cases}$$

as the actual output utilized by controller and $\Delta z(k) = z(k) - z(k-1)$. Therefore, the event-triggered MFAC algorithm for nonlinear systems (1) is established as

$$\hat{\phi}(k) = \begin{cases} \hat{\phi}(k_{t-1}) + \frac{\eta\Delta u(k-1)}{\mu + \Delta u^2(k-1)} \times \\ \quad \left(\Delta z(k) - \hat{\phi}(k-1)\Delta u(k-1)\right), & k = k_t \\ \hat{\phi}(k_{t-1}), & k \in (k_{t-1}, k_t) \end{cases} \tag{7}$$

$$\hat{\phi}(k) = \hat{\phi}(1), \text{ if } \left|\hat{\phi}(k)\right| \le \varepsilon \text{ or } |\Delta u(k-1)| \le \varepsilon \text{or } sign\left(\hat{\phi}(k)\right) \ne sign\left(\hat{\phi}(1)\right) \tag{8}$$

$$u(k) = \begin{cases} u(k_{t-1}) + \frac{\rho\hat{\phi}(k)}{\lambda + \hat{\phi}^2(k)} \times \\ \quad (y_d(k+1) - z(k)), & k = k_t \\ u(k_{t-1}), & k \in (k_{t-1}, k_t) \end{cases} \tag{9}$$

where ε is a positive constant, which is sufficiently small. (8) is the reset algorithm of $\hat{\phi}(k)$ and $\hat{\phi}(1)$ represents its initial value. The choice of μ, λ, η and ρ is that μ, λ satisfy $\mu, \lambda > 0$,

and η, ρ satisfy $0 < \eta, \rho \leq 1$. The factor ε is usually selected as 10^{-5}.

Note that the control algorithm (9) and parameter estimation algorithm (7) consist of the I/O signals and do not involve any model information of (1), which makes it a data-driven control method.

III. Main Results

In this section, the sufficient conditions which can ensure the stability of system (1) subject to DoS attacks will be derived by applying the Lyapunov stability theory. The necessary assumption about PPD is firstly given.

Assumption 5: The sign of $\phi(k)$ keeps unchanged for any instant k and $\Delta u(k) \neq 0$, that is, $\phi(k)$ satisfies $\phi(k) > \bar{\varepsilon} > 0$ or $\phi(k) < -\bar{\varepsilon} < 0$, where $\bar{\varepsilon}$ is a small constant. Note that we only consider that $\phi(k) > \bar{\varepsilon} > 0$ in this paper for the sake of convenience.

Remark 5: Noting that as the control input $u(k)$ increases, the system output $y(k)$ should not decrease, which can be considered as a "quasi-linear" characteristic. This condition is similar to those in model-based control methods that require an invariant sign for control direction. Many systems including water level control systems and temperature control systems, satisfy this assumption.

The main results are concluded in Theorem 1.

Theorem 1: Consider the nonlinear systems (1) satisfying Assumptions 1-2, 5 and apply the event-triggered control scheme (6)-(9). If the controller parameters are chosen as $\mu, \lambda > 0$, $0 < \eta, \rho < 1$, and there exists a K_∞ function $\hbar(k_0, k)$ such that the DoS attack sequence satisfies

$$k - 2f_\Xi(k_0, k) - f_n(k_0, k) \geq \hbar(k_0, k) \tag{10}$$

for any interval $[k_0, k] \subset [0, +\infty)$, where the DoS attacks satisfy Assumptions 3-4, then the tracking error $e(k)$ is bounded as k approaches infinity and the upper bound of $e(k)$ is related to $y_d(k)$. If $y_d(k) = y_d$ is time invariant, then $e(k)$ can converge to zero.

Proof: The boundedness of $\hat{\phi}(k)$ is first proved. According to the reset algorithm (8), if $\left|\hat{\phi}(k)\right| \leq \varepsilon$, or $|\Delta u(k-1)| \leq \varepsilon$, or $sign\left(\hat{\phi}(k)\right) \neq sign\left(\hat{\phi}(1)\right)$, then $\hat{\phi}(k) = \hat{\phi}(1)$, that is, the boundedness of $\hat{\phi}(k)$ can be directly obtained.

If the conditions in (8) do not hold, then define $\tilde{\phi}(k) = \hat{\phi}(k) - \phi(k)$ as the estimation error of $\phi(k)$. According to the estimation algorithm (7), one has $\hat{\phi}(k-1) = \hat{\phi}(k_{t-1})$ for any $k_{t-1} < k \leq k_t$. Similarly, by recalling the control algorithm (9), $u(k-1) = u(k_{t-1})$ can be derived for any $k_{t-1} < k \leq k_t$, which will be applied later in the derivation. Next, the boundedness of $\hat{\phi}(k)$ is discussed in two cases separately in terms of the triggering instants.

Case I: if $k_t = k_{t-1} + 1$, according to Lemma 1, $\Delta y(k_t) = \phi(k_{t-1})\Delta u(k_{t-1})$ holds. Equation (7) becomes

$$\begin{aligned}\hat{\phi}(k_t) = \hat{\phi}(k_{t-1}) &+ \frac{\eta \Delta u(k_t - 1)}{\mu + \Delta u^2(k_t - 1)} \\ &\times \left(\phi(k_{t-1})\Delta u(k_{t-1}) - \hat{\phi}(k_{t-1})\Delta u(k_t - 1)\right)\end{aligned} \tag{11}$$

Subtracting $\phi(k_t)$ from both sides of (11) and recalling the relationship between $\tilde{\phi}(k)$ and $\hat{\phi}(k)$, one has

$$\begin{aligned}\tilde{\phi}(k_t) = \tilde{\phi}(k_{t-1}) &+ \frac{\eta \Delta u(k_t - 1)}{\mu + \Delta u^2(k_t - 1)} \\ &\times \left(\phi(k_{t-1})\Delta u(k_{t-1}) - \hat{\phi}(k_{t-1})\Delta u(k_t - 1)\right) \\ &+ \phi(k_{t-1}) - \phi(k_t)\end{aligned} \tag{12}$$

Taking the absolute value of (12), $\tilde{\phi}(k_t)$ satisfies

$$\left|\tilde{\phi}(k_t)\right| \leq |P(k_{t-1})| \left|\tilde{\phi}(k_{t-1})\right| + 2\bar{b} \tag{13}$$

where $P(k_{t-1}) = 1 - \eta\Delta u(k_{t-1})^2 / \left(\mu + \Delta u(k_{t-1})^2\right)$ and $|\phi(k)| \leq \bar{b}$. Noticing that if we select parameters $\mu > 0$ and $0 < \eta \leq 1$, then $\eta\Delta u^2(k_{t-1}) \leq \Delta u^2(k_{t-1}) \leq \mu + \Delta u^2(k_{t-1})$ holds. Therefore, there exists a positive constant d_1 that satisfies $0 \leq |P(k_{t-1})| \leq d_1 < 1$. (13) yields

$$\begin{aligned}\left|\tilde{\phi}(k_t)\right| &\leq d_1 \left|\tilde{\phi}(k_{t-1})\right| + 2\bar{b} \\ &\leq d_1\left(d_1\left|\tilde{\phi}(k_{t-2})\right| + 2\bar{b}\right) + 2\bar{b} \\ &\leq \cdots \\ &\leq d_1^{t-1}\left|\tilde{\phi}(k_1)\right| + \frac{2\bar{b}}{1 - d_1}\end{aligned}$$

Therefore, $\tilde{\phi}(k_t)$ is bounded. Considering the boundedness of $\phi(k)$, one can conclude that $\hat{\phi}(k_t)$ is bounded for the case of $k_t = k_{t-1} + 1$.

Case II: if $k_t \geq k_{t-1} + 2$, one has $u(k_t - 1) = \cdots = u(k) = \cdots = u(k_{t-1})$ and $\Delta u(k_t - 1) = \cdots = \Delta u(k) = \cdots = \Delta u(k_{t-1} + 1) = 0$ from the control algorithm (9). In addition, recalling the parameter estimation algorithm (7), one has $\left|\tilde{\phi}(k)\right| \leq \left|\tilde{\phi}(k_{t-1})\right| + 2\bar{b}$ for any $k \in [k_{t-1}, k_t)$.

Therefore, in combination with the results in Case I and Case II, it is easy to conclude that $\tilde{\phi}(k)$ is bounded for any instant k. Since $\phi(k) \leq \bar{b}$, the boundedness of $\hat{\phi}(k)$ can be derived by the relationship between $\tilde{\phi}(k)$ and $\hat{\phi}(k)$.

Next, some necessary notations of time instants about the triggering instants and attack intervals are first given, and followed by the boundedness discussion of tracking error $e(k)$. Noting that the interval $[k_i, k_i + \tau_i)$ represents the i-th attack interval, and $[k_i + \tau_i, k_{i+1})$ represents the sleeping interval between two adjacent attack intervals. Hence, the triggering instants in $[k_i + \tau_i, k_{i+1})$ are remarked as $k_{i,1}, k_{i,2}, \cdots, k_{i,t}$. Now, for each interval $[k_i, k_{i+1})_{i \in \mathbb{Z}^+}$, consider the case where the triggering condition (6) is satisfied, such as $k = k_{i,t}$, and choose the Lyapunov function as $V(k_{i,t}) = e(k_{i,t})^2$. Since the triggering condition (6) is satisfied, recalling the control algorithm (9) and the definition of $z(k)$, $e(k_{i,t})$ yields that

$$\begin{aligned}e(k_{i,t}) &= y_d(k_{i,t}) - y(k_{i,t}) \\ &= y_d(k_{i,t}) - y(k_{i,t} - 1) - \phi(k_{i,t} - 1)\Delta u(k_{i,t} - 1)\end{aligned} \tag{14}$$

Furthermore, if $k_{i,t} - 1 = k_{i,t-1}$ is the first triggering instant before instant $k_{i,t}$, one has the following relationship by employing the control algorithm (9)

$$\begin{aligned}\Delta u(k_{i,t-1}) &= u(k_{i,t-1}) - u(k_{i,t-1} - 1) \\ &= \frac{\rho\hat{\phi}(k_{i,t-1})}{\lambda + \hat{\phi}^2(k_{i,t-1})}\left(y_d(k_{i,t-1} + 1) - y(k_{i,t-1})\right)\end{aligned} \tag{15}$$

Substituting the increment of the control algorithm (15) into the tracking error (14), one has

$$e(k_{i,t}) = y_d\left(k_{i,t}\right) - y\left(k_{i,t-1}\right) - \phi\left(k_{i,t-1}\right) \times \frac{\rho\hat{\phi}\left(k_{i,t-1}\right)}{\lambda + \hat{\phi}^2\left(k_{i,t-1}\right)}\left(y_d\left(k_{i,t-1}+1\right) - y\left(k_{i,t-1}\right)\right)$$

Furthermore, recalling the definition of $e(k)$, there is

$$e\left(k_{i,t}\right) = y_d\left(k_{i,t}\right) - y_d\left(k_{i,t-1}\right) + \left(y_d\left(k_{i,t-1}\right) - y\left(k_{i,t-1}\right)\right) - \phi\left(k_{i,t-1}\right)\frac{\rho\hat{\phi}\left(k_{i,t-1}\right)}{\lambda + \hat{\phi}^2\left(k_{i,t-1}\right)} \times \left(\Delta y_d\left(k_{i,t-1}+1\right) + \left(y_d\left(k_{i,t-1}\right) - y\left(k_{i,t-1}\right)\right)\right)$$

Meanwhile, the above equation becomes

$$e\left(k_{i,t}\right) = y_d\left(k_{i,t}\right) - y_d\left(k_{i,t-1}\right) - \frac{\rho\hat{\phi}\left(k_{i,t-1}\right)^2}{\lambda + \hat{\phi}^2\left(k_{i,t-1}\right)}\Delta y_d\left(k_{i,t-1}+1\right) + \left(1 - \frac{\rho\hat{\phi}\left(k_{i,t-1}\right)^2}{\lambda + \hat{\phi}^2\left(k_{i,t-1}\right)}\right)e\left(k_{i,t-1}\right)$$

It yields

$$e\left(k_{i,t}\right) \le Q\left(k_{i,t-1}\right)\nabla y_d^{\max} + Q\left(k_{i,t-1}\right)e\left(k_{i,t-1}\right) \quad (16)$$

where $\nabla y_d^{\max} = \max\left\{\Delta y_d(1), \Delta y_d(2), \cdots, \Delta y_d(k)\right\}$ and $Q\left(k_{i,t-1}\right) = 1 - \rho\hat{\phi}\left(k_{i,t-1}\right)^2 / \left(\lambda + \left|\hat{\phi}\left(k_{i,t-1}\right)\right|^2\right)$. Here, since the actual value of $\phi(k)$ is unknown for controller designer, is replaced by $\hat{\phi}(k)$, which can be estimated by the parameter estimation algorithm (7).

In addition, if $k_{i,t} - 1 \neq k_{i,t-1}$, $e\left(k_{i,t}\right)$ is formulated as the following form along the previous analysis that $\Delta u\left(k_{i,t}-1\right) = \cdots = \Delta u(k) = \cdots = \Delta u\left(k_{i,t-1}+1\right) = 0$,

$$e\left(k_{i,t}\right) = y_d\left(k_{i,t}\right) - y\left(k_{i,t}-1\right) - \phi\left(k_{i,t}-1\right)\Delta u\left(k_{i,t}-1\right)$$

Since $\Delta u\left(k_{i,t}-1\right) = 0$, $e\left(k_{i,t}\right)$ is further rewritten as

$$e\left(k_{i,t}\right) = y_d\left(k_{i,t}\right) - y\left(k_{i,t}-2\right) - \phi\left(k_{i,t}-2\right)\Delta u\left(k_{i,t}-2\right)$$

Also, along the same trajectories, one has

$$e\left(k_{i,t}\right) = y_d\left(k_{i,t}\right) - y\left(k_{i,t-1}\right) - \phi\left(k_{i,t-1}\right)\Delta u\left(k_{i,t-1}\right)$$

Recalling (15), one can obtain the same results as in (16). Meanwhile, according to the boundedness of $\hat{\phi}(k)$ and the reset algorithm (8), there exists a positive constant $\bar{\varepsilon}$ that satisfies $\varepsilon \le \hat{\phi}(k) \le \bar{\varepsilon}$ for any k. Since $\rho \in (0,1]$ and the function $Q(k)$ is decreasing monotonically with respect to $\hat{\phi}(k)$, there exists constants $\lambda, \bar{c}, \underline{c} > 0$ that satisfy

$$\underline{c} = \frac{\rho\varepsilon^2}{\lambda + \varepsilon^2} \le 1 - Q(k) \le \frac{\rho\bar{\varepsilon}^2}{\lambda + \bar{\varepsilon}^2} = \bar{c} < 1 \quad (17)$$

which reveals that $Q(k)$ is also bounded. Recalling the Lyapunov function $V\left(k_{i,t}\right)$ and denoting its derivation is $\Delta V\left(k_{i,t}\right) = e^2\left(k_{i,t}\right) - e^2\left(k_{i,t-1}\right)$, there is

$$\Delta V\left(k_{i,t}\right) = e\left(k_{i,t}\right)^2 - e\left(k_{i,t-1}\right)^2 \le \left(Q\left(k_{i,t-1}\right)\nabla y_d^{\max} + Q\left(k_{i,t-1}\right)e\left(k_{i,t-1}\right)\right)^2 - e\left(k_{i,t-1}\right)^2 \le 2Q\left(k_{i,t-1}\right)^2\left(\nabla y_d^{\max}\right)^2 + \left(2Q\left(k_{i,t-1}\right)^2 - 1\right)V\left(k_{i,t-1}\right)$$

It is clear that the triggering error $\varpi\left(k_t\right)$ is equal to zero at the triggering instant. Hence, one has $2Q^2\left(k_{i,t-1}\right)\left(\nabla y_d^{\max}\right)^2 < \gamma\, e\left(k_{i,t-1}\right)^2 < e\left(k_{i,t-1}\right)^2$ from the triggering condition (6). Accordingly, $V(k)$ follows that

$$V\left(k_{i,t}\right) \le \left(2Q\left(k_{i,t-1}\right)^2 + 1\right)V\left(k_{i,t-1}\right) = \omega_1\left(k_{i,t-1}\right)^{-1}V\left(k_{i,t-1}\right)$$

where $\omega_1\left(k_{i,t-1}\right) = \left(2Q\left(k_{i,t-1}\right)^2 + 1\right)^{-1}$. Furthermore, $V\left(k_{i,t}\right)$ satisfies

$$\begin{aligned} V\left(k_{i,t}\right) &\le \omega_1\left(k_{i,t-1}\right)^{-1}V\left(k_{i,t-1}\right) \\ &\le \omega_1\left(k_{i,t-1}\right)^{-1}\omega_1\left(k_{i,t-2}\right)^{-1}V\left(k_{i,t-2}\right) \\ &\le \cdots \\ &\le \omega_1\left(k_{i,t-1}\right)^{-1} \times \cdots \times \omega_1\left(k_{i,1}\right)^{-1}V\left(k_{i,1}\right) \\ &= \prod_{t'=1}^{t-1}\omega_1\left(k_{i,t'}\right)^{-1}V\left(k_{i,1}\right) \end{aligned}$$

Defining $\bar{\omega}_{1,i} = \min\left\{\omega_1\left(k_{i,1}\right), \omega_1\left(k_{i,2}\right), \cdots, \omega_1\left(k_{i,t-1}\right)\right\} \le 1$, then the above inequation yields

$$V\left(k_{i,t}\right) \le \prod_{t'=1}^{t-1}\omega_1\left(k_{i,t'}\right)^{-1}V\left(k_{i,1}\right) \le \bar{\omega}_{1,i}^{-(t-1)}V\left(k_{i,1}\right) \quad (18)$$

where $k_{i,1}$ denotes the first triggering instant within the sleeping interval $\left[k_i + \tau_i, k_{i+1}\right)$. The second case is the instant when the triggering condition (6) in the interval $\Theta\left[k_i, k_{i+1}\right)$ is not satisfied. Therefore, the control input $u(k)$ remains unchanged according to the updating algorithm (9). Thus, for those holding instants in interval $\left[k_{i,t'}, k_{i,t'+1}\right)_{t'\in\mathbb{Z}^+}$, one has

$$\begin{aligned} e(k) &= y_d(k) - y(k) \\ &= \cdots \\ &= y_d(k) - y\left(k_{i,t'}\right) - \phi\left(k_{i,t'}\right)\Delta u\left(k_{i,t'}\right) \\ &\le Q\left(k_{i,t'}\right)\nabla y_d^{\max} + Q\left(k_{i,t'}\right)e\left(k_{i,t'}\right) \end{aligned}$$

Hence, it is obvious that (18) can be extended as $V(k) \le \bar{\omega}_{1,i}^{-(k-k_i-\tau_i)}V\left(k_i+\tau_i+1\right)$ for the interval $\left[k_i+\tau_i, k_{i+1}\right)$, where $k_i + \tau_i + 1$ denotes the first sampling instant in this sleeping interval.

For other cases, k belongs to the attack interval $[k_i, k_i+\tau_i)$, which means that the event-triggered mechanism is interrupted within the attack intervals. Similarly, choosing the Lyapunov function as $V(k) = e^2(k)$ for $[k_i, k_i+\tau_i)$. Since $u(k) = u(k_i)$, then one has $\Delta u(k-1) = 0$ and the tracking error $e(k)$ satisfies that

$$\begin{aligned} e(k) &= y_d(k) - y(k) \\ &= y_d(k) - y(k-1) - \phi(k-1)\Delta u(k-1) \\ &= \Delta y_d(k) + e(k-1) \end{aligned}$$

Therefore, the derivation of Lyapunov function becomes

$$\begin{aligned}\Delta V(k) &= V(k) - V(k-1)\\ &= e(k)^2 - e(k-1)^2\\ &\le 2\Delta y_d(k)^2 + e(k-1)^2\end{aligned}$$

Meanwhile, there is

$$\begin{aligned}V(k) &\le 2V(k-1) + \omega_2(k)\\ &\le 2\left(2V(k-2) + \omega_2(k-1)\right) + \omega_2(k)\\ &\le \cdots\\ &\le 2^{k-k_i} V(k_i) + \sum_{i'=0}^{k-k_i-1} 2^{i'} \omega_2\left(k-i'\right)\end{aligned} \tag{19}$$

where $\omega_2(k) = 2\Delta y_d^2(k)$ and k_i represents the first sampling within this attack interval. Recalling the upper bound of $\Delta y_d(k)$, one has $\omega_2(k) \le \bar{\omega}_2 = 2\left(\nabla y_d^{\max}\right)^2$ and

$$\begin{aligned}\sum_{i'=0}^{k-k_i-1} 2^{i'} \omega_2\left(k-i'\right) &\le \sum_{i'=0}^{k-k_i-1} 2^{i'} \bar{\omega}_2\\ &\le \bar{\omega}_2 \sum_{i'=0}^{k-k_i-1} 2^{i'} = \bar{\omega}_2\left(2^{k-k_i} - 1\right)\end{aligned}$$

Since the length of each attack interval is bounded, we can derive the boundedness of $\bar{\omega}_2\left(2^{k-k_i} - 1\right)$ and define its boundary $M_{\max}$. Therefore, combining (18) and (19), $V(k)$ satisfies $V(k) \le 2^{-\Theta(k_i,k)+\Xi(k_i,k)} V(k_i) + M_{\max}$ for interval $\left[k_i, k_{i+1}\right)_{i\in\mathbb{Z}^+}$. Noticing that the Assumptions 3-4 about attack frequency and duration are satisfied for any time interval, then one has

$$V(k) \le 2^{-\Theta(0,k)+\Xi(0,k)} V(0) + M_{\max}$$

Combing with Assumptions 3-4, it yields that

$$\begin{aligned}V(k) &\le V(0)\, 2^{-\Theta(0,k)+\Xi(0,k)} + M_{\max}\\ &\le V(0)\, 2^{2\zeta_\Xi + 2f_\Xi(0,k) + n(0,k) - k} + M_{\max}\\ &\le \Upsilon 2^{2f_\Xi(0,k) + f_n(0,k) - k} + M_{\max}\end{aligned} \tag{20}$$

where $\Upsilon = V(0)\, 2^{2\zeta_\Xi + \kappa_n}$. From (10), $V(k)$ yields that

$$\begin{aligned}V(k) &\le V(0)\, 2^{-\Theta(0,k)+\Xi(0,k)} + M_{\max}\\ &\le V(0)\, 2^{2\zeta_\Xi + 2f_\Xi(0,k) + n(0,k) - k} + M_{\max}\\ &\le \Upsilon 2^{-\hbar(0,k)} + M_{\max}\end{aligned}$$

Considering the definition of function $\hbar(0,k)$, $V(k)$ satisfies that $0 \le \lim_{k\to\infty} V(k) \le M_{\max}$. The upper bound of the final tracking error is restricted by $y_d(k)$. In other words, if $y_d(k) = y_d$ is a constant, $e(k)$ will approaches zero as k approaches infinity. Therefore, one has proved the boundedness of $e(k)$. This is the end of the proof. ∎

Remark 6: When the malicious attacks are serious, the event-triggered mechanism may be reduced to a fixed time-triggered mechanism. It is seen that compared with the time-triggered mechanism, the event-triggered mechanism is still superior in resource utilization. In a word, since the triggering condition is judged by the control index of tracking error, its convergence will be guaranteed preferentially.

IV. Compensation Algorithm Design

The results in Theorem 2 show that under the MFAC scheme, system (1) still maintains well stability performance even if the existence of intermittent DoS attacks. Considering the channel blocking brought by DoS attacks, the data transmission will inevitably be interfered with, which motivates the design of compensation scheme.

One natural compensation strategy is to assign estimation capabilities to the MFAC algorithm, so that the estimated value $\hat{y}(k)$ can be applied to replace the lost output $y(k)$ and then reconstruct the control input during the attack intervals. Therefore, denote

$$r(k) = \begin{cases} y(k), & k \in \Theta(k_0, k)\\ \hat{y}(k), & k \in \Xi(k_0, k)\end{cases}$$

as the actual output for the compensation controller and the MFAC algorithm is redesigned as follows

$$\begin{aligned}\hat{\phi}(k) &= \hat{\phi}(k-1) + \frac{\eta \Delta u(k-1)}{\mu + \Delta u^2(k-1)}\\ &\quad \times \left(\Delta r(k) - \hat{\phi}(k-1)\Delta u(k-1)\right)\end{aligned} \tag{21}$$

$$u(k) = u(k-1) + \frac{\rho\hat{\phi}(k)}{\lambda + \hat{\phi}^2(k)}\left(y_d(k+1) - r(k)\right) \tag{22}$$

where $\Delta r(k) = r(k) - r(k-1)$. $\hat{y}(k)$ denotes the estimated value and it can be obtained by

$$\hat{y}(k) = r(k-1) + \hat{\phi}(k-1)\Delta u(k-1)$$

Noting that the former algorithm in (7)-(9) employs the previous output $y(k-1)$ to construct the input during the attack intervals, while it is replaced by $\hat{y}(k)$ in the compensation algorithm (21)-(22). The main results of this section are given as follows.

Theorem 2: Consider the system (1) satisfying the Assumptions 1-2, 5 and apply the compensation MFAC (8), (21)-(22). If μ, η are chosen as $\mu > 0$, $0 < \eta < 1$ and if there exists any time instant that (1) is not attacked in interval $[k_0, k] \subset [0, +\infty)$, then $e(k)$ is bounded as k approaches infinity.

Proof: The proof of the boundedness of $\hat{\phi}(k)$ is similar to the process in Theorem 1 and the details are omitted here. For any two adjacent sampling instants $k_{t-1}, k_t \in \Theta$, one has $r(k_{t-1}+1) = y(k_{t-1}) + \hat{\phi}(k_{t-1})\Delta u(k_{t-1})$ and

$$\begin{aligned}r(k_{t-1}+2) = y(k_{t-1}) &+ \hat{\phi}(k_{t-1})\Delta u(k_{t-1})\\ &+ \hat{\phi}(k_{t-1}+1)\Delta u(k_{t-1}+1)\end{aligned}$$

Next, for any $k_{t-1} < k < k_t$, $r(k)$ follows

$$\begin{aligned}r(k) = y &+ \hat{\phi}(k_{t-1})\Delta u(k_{t-1})\\ &+ \cdots + \hat{\phi}(k-1)\Delta u(k-1)\end{aligned}$$

The control algorithm (22) is governed by

$$u(k) = \begin{cases} u(k-1) + \dfrac{\rho\hat{\phi}(k)}{\lambda + \hat{\phi}^2(k)}\left(\Delta y_d(k+1) + e(k)\right),\\ \qquad\qquad k = k_{t-1} \text{ or } k = k_t\\ u(k-1) + \dfrac{\rho\hat{\phi}(k)}{\lambda + \hat{\phi}^2(k)}\left(y_d(k+1) - y_d(k_{t-1})\right.\\ \qquad \left. + e(k_{t-1}) - \hat{\phi}(k_{t-1})\Delta u(k_{t-1}) - \right.\\ \cdots - \left.\hat{\phi}(k-1)\Delta u(k-1)\right), \quad k_{t-1} < k < k_t\end{cases} \tag{23}$$

From (23), $\Delta u\left(k_{t-1}\right)$ becomes

$$\begin{aligned}\Delta u\left(k_{t-1}\right) &= \frac{\rho\hat{\phi}\left(k_{t-1}\right)}{\lambda+\hat{\phi}^2\left(k_{t-1}\right)}\left(\Delta y_d\left(k_{t-1}+1\right)+e\left(k_{t-1}\right)\right)\\ &\leq \frac{\rho\hat{\phi}\left(k_{t-1}\right)}{\lambda+\hat{\phi}^2\left(k_{t-1}\right)}\left(e\left(k_{t-1}\right)+2c\right)\end{aligned}$$

where c is the upper bound of $|y_d(k)|$. Along the similar trajectory, one has

$$\begin{aligned}\Delta u\left(k_{t-1}+1\right) &= \frac{\rho\hat{\phi}\left(k_{t-1}+1\right)}{\lambda+\hat{\phi}^2\left(k_{t-1}+1\right)}\\ &\quad\times\left(y_d\left(k_{t-1}+2\right)-y_d\left(k_{t-1}\right)+e\left(k_{t-1}\right)\right.\\ &\quad\left.-\hat{\phi}\left(k_{t-1}\right)\Delta u\left(k_{t-1}\right)\right)\\ &\leq \frac{2c\rho\hat{\phi}\left(k_{t-1}+1\right)}{\lambda+\hat{\phi}^2\left(k_{t-1}+1\right)}Q\left(k_{t-1}\right)\\ &\quad+\frac{\rho\hat{\phi}\left(k_{t-1}+1\right)c\left(k_{t-1}\right)}{\lambda+\hat{\phi}^2\left(k_{t-1}+1\right)}e\left(k_{t-1}\right)\end{aligned}$$

Furthermore, for any $k_{t-1}<k<k_t$, $\Delta u(k)$ satisfies

$$\begin{aligned}\Delta u\left(k\right) &\leq \frac{\rho\hat{\phi}\left(k\right)\prod_{i=k_{t-1}}^{k-1}Q\left(i\right)}{\lambda+\hat{\phi}^2\left(k\right)}2t+\frac{\rho\hat{\phi}\left(k\right)\prod_{i=k_{t-1}}^{k-1}Q\left(i\right)}{\lambda+\hat{\phi}^2\left(k\right)}e\left(k_{t-1}\right)\\ &= \frac{\rho\hat{\phi}\left(k\right)\prod_{i=k_{t-1}}^{k-1}Q\left(i\right)}{\lambda+\hat{\phi}^2\left(k\right)}\left(2c+e\left(k_{t-1}\right)\right)\end{aligned}\tag{24}$$

According to Lemma 1, $y(k)$ yields

$$\begin{aligned}y\left(k\right) &= y\left(k-1\right)+\phi\left(k-1\right)\Delta u\left(k-1\right)=\cdots\\ &= y\left(k_{t-1}\right)+\phi\left(k_{t-1}\right)\Delta u\left(k_{t-1}\right)+\cdots\\ &\quad+\phi\left(k-1\right)\Delta u\left(k-1\right)\end{aligned}\tag{25}$$

Combing (24)-(25) and replacing $\phi(k)$ with the estimated value $\hat{\phi}(k)$, $e(k)$ becomes

$$\begin{aligned}e\left(k\right) &= y_d\left(k\right)-y_d\left(k_{t-1}\right)+e\left(k_{t-1}\right)\\ &\quad-\phi\left(k_{t-1}\right)\Delta u\left(k_{t-1}\right)-\cdots-\phi\left(k-1\right)\Delta u\left(k-1\right)\\ &\leq 2c+e\left(k_{t-1}\right)-\frac{\rho\hat{\phi}^2\left(k_{t-1}\right)}{\lambda+\hat{\phi}^2\left(k_{t-1}\right)}\left(2c+e\left(k_{t-1}\right)\right)\\ &\quad-\cdots-\frac{\rho\hat{\phi}^2\left(k-1\right)\prod_{i=k_{t-1}}^{k-2}Q\left(i\right)}{\lambda+\hat{\phi}^2\left(k-1\right)}\left(2c+e\left(k_{t-1}\right)\right)\\ &\leq \left(2t+e\left(k_{t-1}\right)\right)\left(1-\sum_{k=k_{t-1}}^{k-1}\left(\left(1-Q\left(k\right)\right)\prod_{i=k_{t-1}}^{k-1}Q\left(i\right)\right)\right)\end{aligned}\tag{26}$$

Recalling (17), the following inequality holds

$$\begin{aligned}0 &\leq \underline{c}+\underline{c}\left(1-\bar{c}\right)+\cdots+\underline{c}(1-\bar{c})^{k-k_{t-1}}\\ &\leq \sum_{k=k_{t-1}}^{k-1}\left(\left(1-Q\left(k\right)\right)\prod_{i=k_{t-1}}^{k-1}Q\left(i\right)\right)\\ &\leq c+\bar{c}\left(1-\underline{c}\right)+\cdots+\bar{c}\left(1-\underline{c}\right)^{k-k_{t-1}}\end{aligned}\tag{27}$$

where $\underline{c}+\underline{c}\left(1-\bar{c}\right)+\cdots+\underline{c}(1-\bar{c})^{k-k_{t-1}}\frac{c}{\bar{c}}<1$.

According to (27), there exists a positive constant $d'(k-k_{t-1})$ such that

$$\begin{aligned}&\left|1-\sum_{k=k_{t-1}}^{k-1}\left(\left(1-Q\left(k\right)\right)\prod_{i=k_{t-1}}^{k-1}Q\left(i\right)\right)\right|\\ &\quad\leq\left|1-\left(\underline{c}+\underline{c}\left(1-\bar{c}\right)+\cdots+\underline{c}(1-\bar{c})^{k-k_{t-1}}\right)\right|\\ &\quad= d'\left(k-k_{t-1}\right)<1\end{aligned}\tag{28}$$

Considering (28) and taking the absolute values of both sides of (26), one has

$$\left|e\left(k\right)\right|\leq 2cd'\left(k-k_{t-1}\right)+d'\left(k-k_{t-1}\right)\left|e\left(k_{t-1}\right)\right|\tag{29}$$

Since $d'(k-k_{t-1})<1$, the tracking error $e(k)$ is bounded, which implies that the compensation mechanism can guarantee the convergence of the tracking error when (1) is not always attacked for the whole time interval. Moreover, along the similar analysis method, the convergence rate of $e(k)$ in scheme (7)-(9) is

$$\begin{aligned}\left|e\left(k\right)\right| &\leq \left|1-\frac{\rho\hat{\phi}^2\left(k_{i-1}\right)}{\lambda+\hat{\phi}^2\left(k_{i-1}\right)}\right|\left|e\left(k_{i-1}\right)+2c\right|\\ &\leq \left(1-\underline{c}\right)\left|e(k_{i-1})\right|+2c(1-\underline{c})\end{aligned}\tag{30}$$

Comparing the results in (29) and (30), it is observed that $e(k)$ in (29) converges faster and achieves a smaller upper bound, which reveals the effectiveness of the compensation algorithm. This ends the proof. ■

V. Simulation Results

In this section, a set of simulations including a numerical example and a LFC example for multi-area power system are carried out to confirm the validity of the proposed schemes under the intermittent DoS attacks.

A. Numerical Example

The following SISO nonlinear system is test

$$\begin{aligned}&y\left(k+1\right)\\ &=\begin{cases}\dfrac{y\left(k\right)}{1+y^2(k)}+u^3(k), & 0<k\leq 200\\ \dfrac{\left(\begin{array}{l}y\left(k\right)y\left(k-1\right)y\left(k-2\right)u\left(k-1\right)\\ \times\left(y\left(k-2\right)-1\right)+a\left(k\right)u\left(k\right)\end{array}\right)}{1+y^2(k-1)+y^2(k-2)}, & 200<k\leq 400\end{cases}\end{aligned}$$

where $a(k)=0.5\times(-1)^{round(k/200)}$. The structure, parameters and order of the above system are all time-varying. It is worth noting that the system model presented here is only to generate necessary I/O data to support the operation of the simulation.

The desired time-varying trajectory is selected as

$$\begin{aligned}&y_d\left(k\right)\\ &=\begin{cases}0.5\times(-1)^{round(k/200)}, & 0<k\leq 100\\ 0.5\sin\left(k\pi/100\right)+0.3\cos\left(k\pi/50\right), & 100<k\leq 400\end{cases}\end{aligned}$$

The controller parameters are chosen as: $\eta=1$, $\mu=1$, $\rho=0.6$, $\lambda=0.1$, $\varepsilon=10^{-5}$, $\hat{\phi}(1)=0.5$. The initial conditions are

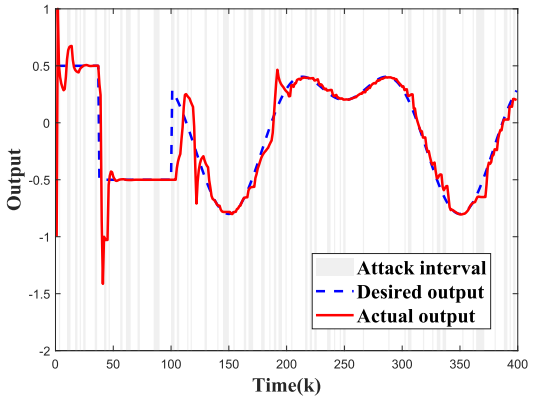

Fig. 4. System output under DoS attacks.

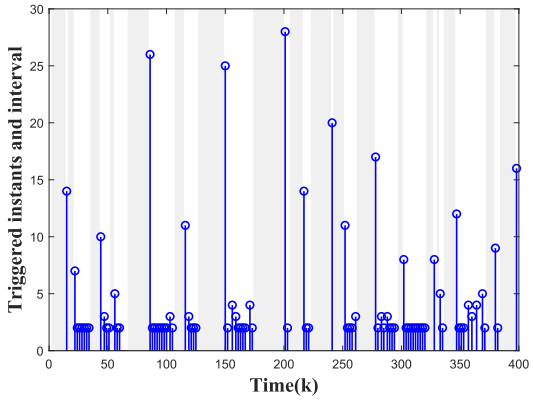

Fig. 6. Triggering instants and intervals.

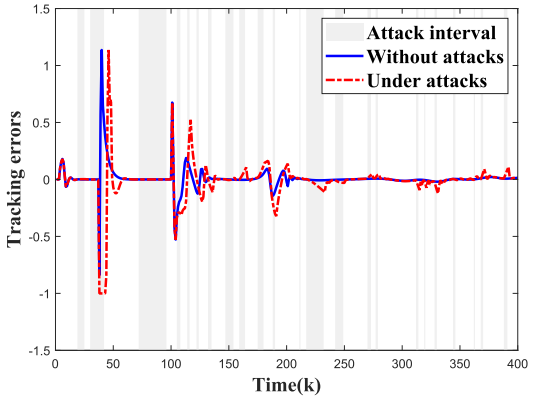

Fig. 5. Comparison of tracking errors with and without DoS attacks.

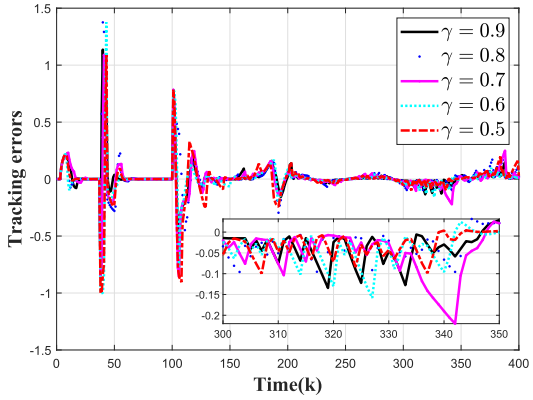

Fig. 7. Tracking errors under the different triggering parameters.

$y(1) = -1$, $y(2) = 1$, $y(3) = 0.5$, $u(1) = u(2) = 0$. Consider a attack sequence as $n(k_0, k) \leq 1 + k - k_0 + 0.5\sqrt{k - k_0}$ and $\Xi(k_0, k) \leq 1 + k - k_0 - \left(0.2(k - k_0) + 0.02(k - k_0)^2\right)$, where $n(k_0, k)$ and $\Xi(k_0, k)$ can satisfy the Assumptions 3-4. The function $\hbar(k_0, k)$ that satisfies Theorem 1 is selected as

$$\hbar(0, k) = -2\left(k - \left(0.2k + 0.02(k)^2\right)\right) - \left(k + 0.5\sqrt{k}\right)$$

The response of the system output is plotted in Fig. 4 and there were 23 attacks with a total duration of 89 sampling instants within the time interval $[0, 400]$, which means that 22.25% of data transfers failed. The results in Fig. 4 reveal that the proposed event-triggered MFAC can still track the desired output despite the intermittent attacks, which reflects the ability of MFAC to deal with the attacks.

Fig. 5 plots the convergence curves of tracking error in the cases of attack and non-attack respectively. The results show that both two curves converge to zero, and fluctuate within a small range. Nevertheless, it is also observed that the error curve under the attacks fluctuates more dramatically and the smoothness is poorer than another case. Meanwhile, by calculating the integral of absolute value of error (IAE, $\sum_{k=1}^{400} |e(k)|$) and the integral of squared error (ISE, $\sum_{k=1}^{400} |e(k)|^2$), it is obtained that the criterions under attacks are IAE = 31.22 and ISE = 12.74, and the criterions under the non-attacks are IAE = 24.84 and ISE = 4.99, which declares the adverse impact of the DoS attacks on the system stability.

In addition, we are interested in the validity of the presented event-triggered strategy. In Fig. 6, the triggering instants and intervals are plotted. In detail, the position of the matchstick represents the time instant the "event" occurred, and the height of the matchstick represents the interval between two adjacent triggered "events". Within the time interval $[0, 400]$, "events" were triggered 108 times and the average triggering interval is 3.7 sampling instants, which verifies a 73% saving in transmission resource. Fig. 6 shows that compared to the triggering scheme based on the fixed sampling period, the proposed flexible triggering mechanism can significantly reduce the numbers of information transmission.

The influence brought by the selection of triggering parameters on the convergence rate of the tracking error is studied in Fig. 7. The results declare that the several curves almost coincide around 0 curve, which indicates that the selection of triggering parameters does not significantly affect the convergence performance.

Furthermore, the effectiveness of the compensation algorithm is verified in Fig. 8. By calculating the values of the criterion function, the criterions under the compensation scheme are IAE = 26.79 and ISE = 5.36. More specifically, it is seen that the initial method performs no tracking capability during the attack intervals, leaving the system output unchanged. By contrast, the compensation method can still track the desired trajectory by taking advantage of the estimation abilities.

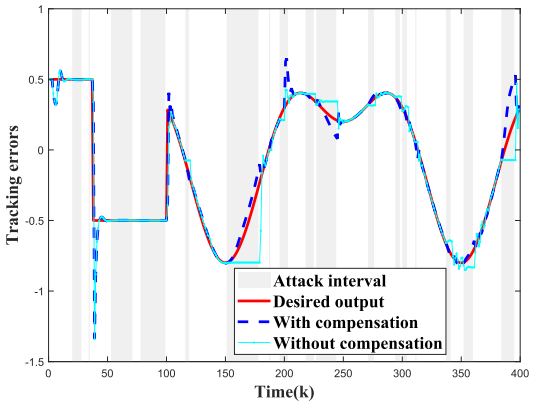

Fig. 8. Comparison of tracking errors between two control schemes.

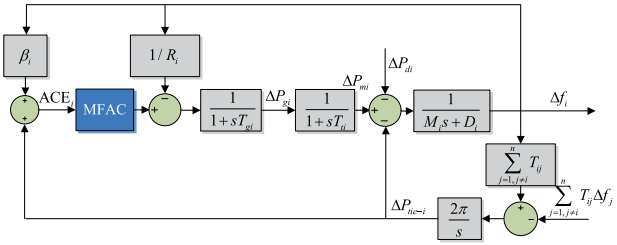

Fig. 9. LFC structure of multi-area power systems.

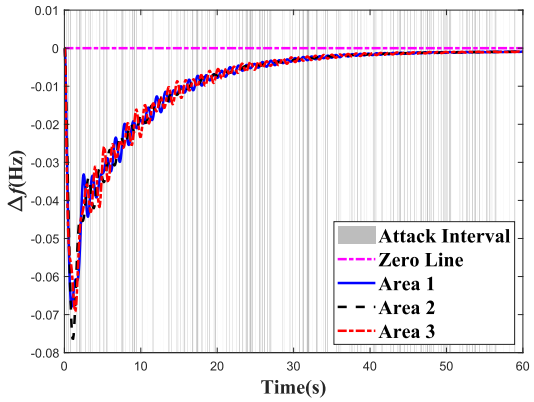

Fig. 10. Frequency response Δf of power system.

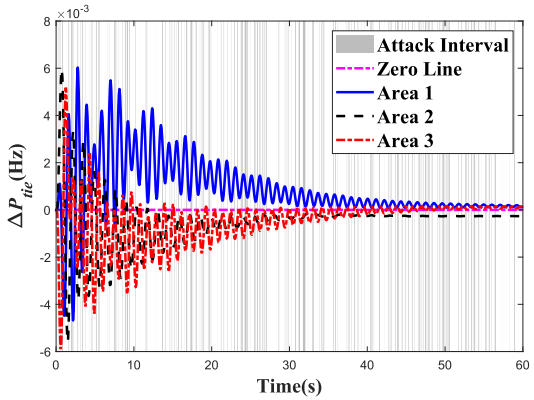

Fig. 11. Tie line power deviation response ΔP_{tie} of power system.

B. LFC for Three-Area Power System

To further verify the validity of the proposed methods and also explore the impact of DoS attacks and event-triggered mechanism on the system, the LFC example for three-area power system is studied. The main objective is to establish a control scheme can guarantee the convergence of the area control error. The structure of LFC is shown in Fig. 9 and the definitions of the signals can refer to the TABLE I in [44]. For the sampling period T, the discrete-time form of the $i-$th power system is as

$$\begin{cases} x_i(k+1) = G_i x_i(k) + H_i u(k) + W_i \omega_i(k) \\ y_i(k) = C_i x_i(k) \end{cases}$$

where $x_i(k) = \left[\Delta f_i \ \Delta P_{\text{tie-}i} \ \Delta P_{\text{mi}} \ \Delta P_{\text{gi}}\right]^T$, $y_i(k) = \text{ACE}_i$, $u(k)$ denote the system state, the output and the control input respectively, and $\omega_i^T(k) = \left[\Delta P_{\text{di}} \sum_{i=1, j\neq i}^{N} T_{ij} \Delta f_j\right]$ can be viewed as an external disturbance. In addition, the meanings of G_i, H_i, W_i, C_i and the system parameters can be found in [44], which are omitted here for space saving.

The operation time is 60s and sampling period $T = 0.005$. The parameters of the MFAC are the same and selected as $\eta = 0.4$, $\mu = 1.4$, $\rho = 2.7$ and $\lambda = 2.5$. The initial state of the system is 0 and $\hat{\phi}(1:3, 1:2) = 0.1$. The triggering parameter is $\gamma = 0.7$ and the attack function $\hbar(0, k)$ is

$$\hbar(0,k) = -4\left(k - \left(2k + k^2\right)\right) - \left(2k + 5\sqrt{k}\right)$$

The simulation results are shown in Figs. 10-14. Figs. 10-11 plot the response curves of Δf and ΔP_{tie} under the DoS attacks. Gray areas in the figures represent the attack intervals. It is shown that although the data transmission is blocked, the proposed data-driven control scheme can guarantee that the curves converge to near 0.

Employing areas 1-2 as examples, Figs. 12-13 show the triggering instants and intervals during transmission. For the time-based mechanism, the triggering interval is 1. Accordingly, the number of "events" under the event-triggered mechanism is 4107, 6937, 8620 in a total of 12000 sampling instants, respectively. The average triggering interval is 2.92, 1.73 and 1.39 respectively. Furthermore, from the point view of data transmission, the proposed event-triggered mechanism saves 65.77%, 42.19%, 28.17% bandwidth resources respectively. These results have proved that the proposed event-triggered mechanism performs well in reducing the unnecessary transmission.

In addition, the effectiveness of the compensation scheme is verified in Fig. 14. It is seen that the curve of Δf can converge to 0 under different control schemes. Nevertheless, it is observed that compared with the curve under the compensation scheme, the original control scheme achieves a slower convergence rate and a larger static tracking error. This illustrates that the compensation design is effective in dealing with the DoS attacks.

All the simulation results in Figs. 4-8 and Figs. 10-14 have shown that the proposed event-triggered MFAC can effectively handle the adverse effects of external attacks in the transmission channels. Furthermore, the event-triggered

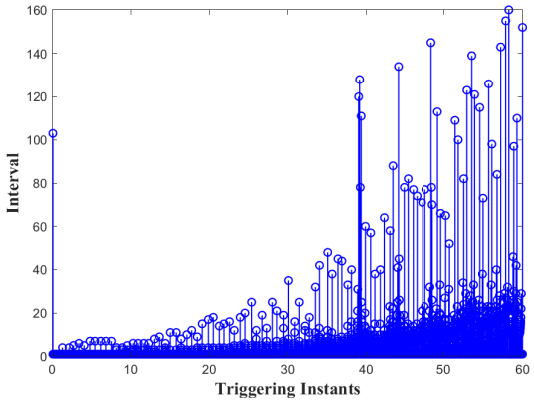

Fig. 12. Triggering instants and the interval for area 1.

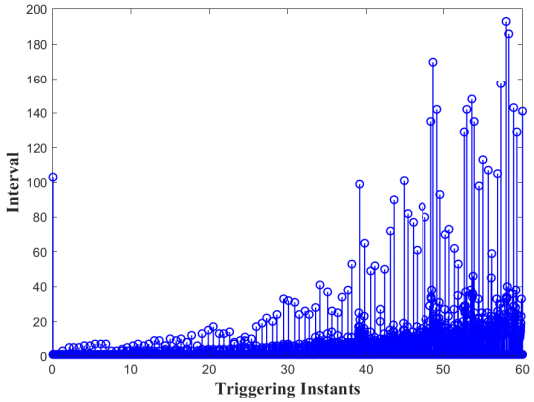

Fig. 13. Triggering instants and the interval for area 2.

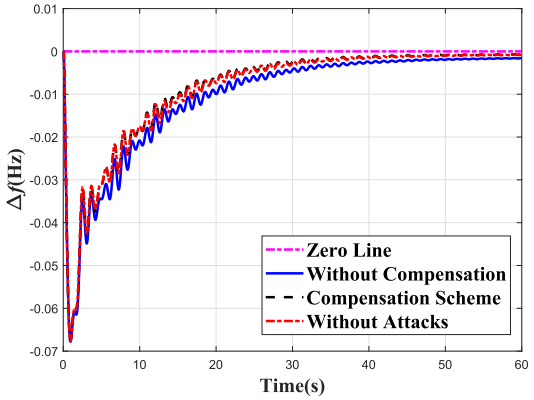

Fig. 14. Comparison of Δf under different control schemes.

strategy can improve the utilization rate of the system bandwidth while maintaining the system performance.

VI. Conclusion

The event-triggered data-driven MFAC is designed for nonlinear systems under DoS attacks in the paper. Considering the security of CPSs, an intermittent attack sequence is formulated, which is only constrained by their frequency and duration. To save energy consumption, an event-triggered communication scheme was constructed without decreasing the stability performance. Furthermore, to counteract the negative influence of malicious attacks on system, the estimated output is applied to replace the actual value within the attack intervals. The analysis and illustrative examples have proved the effectiveness of the proposed algorithms.

References

[1] A. W. Colombo, S. Karnouskos, O. Kaynak, Y. Shi, and S. Yin, "Industrial cyberphysical systems: A backbone of the fourth industrial revolution," *IEEE Ind. Electron. Mag.*, vol. 11, no. 1, pp. 6–16, Mar. 2017.

[2] Y. Tang, D. Zhang, D. W. C. Ho, and F. Qian, "Tracking control of a class of cyber-physical systems via a FlexRay communication network," *IEEE Trans. Cybern.*, vol. 49, no. 4, pp. 1186–1199, Apr. 2019.

[3] D. Ding, Q.-L. Han, Z. Wang, and X. Ge, "A survey on model-based distributed control and filtering for industrial cyber-physical systems," *IEEE Trans. Ind. Informat*, vol. 15, no. 5, pp. 2483–2499, May 2019.

[4] Y. Zhang, Z. Zhu, and J. Lv, "CPS-based smart control model for shopfloor material handling," *IEEE Trans. Ind. Informat.*, vol. 14, no. 4, pp. 1764–1775, Apr. 2018.

[5] S. S.-D. Xu, H.-C. Huang, Y.-C. Kung, and Y.-Y. Chu, "A networked multirobot CPS with artificial immune fuzzy optimization for distributed formation control of embedded mobile robots," *IEEE Trans. Ind. Informat.*, vol. 16, no. 1, pp. 414–422, Jan. 2020.

[6] Y. Li and K. Yu, "Adaptive fuzzy decentralized sampled-data control for large-scale nonlinear systems," *IEEE Trans. Fuzzy Syst.*, vol. 30, no. 6, pp. 1809–1822, Jun. 2022.

[7] X. Xie, C. Wei, Z. Gu, and K. Shi, "Relaxed resilient fuzzy stabilization of discrete-time Takagi–Sugeno systems via a higher order time-variant balanced matrix method," *IEEE Trans. Fuzzy Syst.*, vol. 30, no. 11, pp. 5044–5050, Nov. 2022.

[8] D. Ding, Z. Wang, Q.-L. Han, and G. Wei, "Security control for discrete-time stochastic nonlinear systems subject to deception attacks," *IEEE Trans. Syst., Man, Cybern., Syst.*, vol. 48, no. 5, pp. 779–789, May 2016.

[9] C. Z. Bai, F. Pasqualetti, and V. Gupta, "Data-injection attacks in stochastic control systems: Detectability and performance tradeoffs," *Automatica*, vol. 82, pp. 251–260, Aug. 2017.

[10] J. Liu, M. Yang, E. Tian, J. Cao, and S. Fei, "Event-based security control for state-dependent uncertain systems under hybrid-attacks and its application to electronic circuits," *IEEE Trans. Circuits Syst. I, Reg. Papers*, vol. 66, no. 12, pp. 4817–4828, Dec. 2019.

[11] E. Mousavinejad, F. Yang, Q.-L. Han, and L. Vlacic, "A novel cyber attack detection method in networked control systems," *IEEE Trans. Cybern.*, vol. 48, no. 11, pp. 3254–3264, Nov. 2018.

[12] G. K. Befekadu, V. Gupta, and P. J. Antsaklis, "Risk-sensitive control under Markov modulated denial-of-service (DoS) attack strategies," *IEEE Trans. Autom. Control*, vol. 60, no. 12, pp. 3299–3304, Dec. 2015.

[13] C. D. Persis and P. Tesi, "Input-to-state stabilizing control under denial-of-service," *IEEE Trans. Autom. Control*, vol. 60, no. 11, pp. 2930–2944, Nov. 2015.

[14] C. De Persis and P. Tesi, "Resilient control under denial-of-service," *IFAC Proc. Volumes*, vol. 47, no. 3, pp. 134–139, 2014.

[15] L. An and G.-H. Yang, "Decentralized adaptive fuzzy secure control for nonlinear uncertain interconnected systems against intermittent DoS attacks," *IEEE Trans. Cybern.*, vol. 49, no. 3, pp. 827–838, Mar. 2019.

[16] W. Chen, D. Ding, H. Dong, and G. Wei, "Distributed resilient filtering for power systems subject to denial-of-service attacks," *IEEE Trans. Syst., Man, Cybern., Syst.*, vol. 49, no. 8, pp. 1688–1697, Aug. 2019.

[17] S. Hu, Z. Cheng, D. Yue, C. Dou, and Y. Xue, "Bandwidth allocation-based switched dynamic triggering control against DoS attacks," *IEEE Trans. Syst., Man, Cybern. Syst.*, vol. 51, no. 10, pp. 6050–6061, Oct. 2021.

[18] Y. Yang, W. Wang, L. Liu, K. Dev, and N. M. F. Qureshi, "AoI optimization in the UAV-aided traffic monitoring network under attack: A Stackelberg game viewpoint," *IEEE Trans. Intell. Transp. Syst.*, early access, Mar. 22, 2022, doi: 10.1109/TITS.2022.3157394.

[19] H. Liu, "SINR-based multi-channel power schedule under DoS attacks: A Stackelberg game approach with incomplete information," *Automatica*, vol. 100, pp. 274–280, Feb. 2019.

[20] K. Ding, X. Ren, D. E. Quevedo, S. Dey, and L. Shi, "Defensive deception against reactive jamming attacks in remote state estimation," *Automatica*, vol. 113, Mar. 2020, Art. no. 108680.

[21] Y. Li, Y.-X. Li, and S. Tong, "Event-based finite-time control for nonlinear multi-agent systems with asymptotic tracking," *IEEE Trans. Autom. Control*, early access, Aug. 9, 2022, doi: 10.1109/TAC.2022.3197562.

[22] S. Liu, B. Niu, G. Zong, X. Zhao, and N. Xu, "Data-driven-based event-triggered optimal control of unknown nonlinear systems with input constraints," *Nonlinear Dyn.*, vol. 109, no. 2, pp. 891–909, May 2022.
[23] F. Tang, B. Niu, G. Zong, X. Zhao, and N. Xu, "Periodic event-triggered adaptive tracking control design for nonlinear discrete-time systems via reinforcement learning," *Neural Netw.*, vol. 154, pp. 43–55, Oct. 2022.
[24] J. Sun, J. Yang, S. Li, and W. X. Zheng, "Sampled-data-based event-triggered active disturbance rejection control for disturbed systems in networked environment," *IEEE Trans. Cybern.*, vol. 49, no. 2, pp. 556–566, Feb. 2019.
[25] J. Zhang and G. Feng, "Event-driven observer-based output feedback control for linear systems," *Automatica*, vol. 50, no. 7, pp. 1852–1859, 2014.
[26] Y. Xie and Z. Lin, "Event-triggered global stabilization of general linear systems with bounded controls," *Automatica*, vol. 107, pp. 241–254, Sep. 2019.
[27] X. Liu, X. Su, P. Shi, C. Shen, and Y. Peng, "Event-triggered sliding mode control of nonlinear dynamic systems," *Automatica*, vol. 112, Feb. 2020, Art. no. 108738.
[28] L. Wu, Y. Gao, J. Liu, and H. Li, "Event-triggered sliding mode control of stochastic systems via output feedback," *Automatica*, vol. 82, pp. 79–92, Aug. 2017.
[29] K. Hashimoto, S. Adachi, and D. V. Dimarogonas, "Event-triggered intermittent sampling for nonlinear model predictive control," *Automatica*, vol. 81, pp. 148–155, Jul. 2017.
[30] Z. Sun, L. Dai, Y. Xia, and K. Liu, "Event-based model predictive tracking control of nonholonomic systems with coupled input constraint and bounded disturbances," *IEEE Trans. Autom. Control*, vol. 63, no. 2, pp. 608–615, Feb. 2018.
[31] T. Liu and Z. P. Jiang, "A small-gain approach to robust event-triggered control of nonlinear systems," *IEEE Trans. Autom. Control*, vol. 60, no. 8, pp. 2072–2085, Aug. 2015.
[32] M. Abdelrahim, R. Postoyan, J. Daafouz, and D. Nešić, "Robust event-triggered output feedback controllers for nonlinear systems," *Automatica*, vol. 75, pp. 96–108, Jan. 2017.
[33] S. Hu, D. Yue, X. Xie, X. Chen, and X. Yin, "Resilient event-triggered controller synthesis of networked control systems under periodic DoS jamming attacks," *IEEE Trans. Cybern.*, vol. 49, no. 12, pp. 4271–4281, Dec. 2018.
[34] W. Xu, D. W. C. Ho, J. Zhong, and B. Chen, "Event/self-triggered control for leader-following consensus over unreliable network with DoS attacks," *IEEE Trans. Neural Netw. Learn. Syst.*, vol. 30, no. 10, pp. 3137–3149, Oct. 2019.
[35] Z. Hou and S. Xiong, "On model-free adaptive control and its stability analysis," *IEEE Trans. Autom. Control*, vol. 64, no. 11, pp. 4555–4569, Nov. 2019.
[36] Z. Hou and S. Jin, "A novel data-driven control approach for a class of discrete-time nonlinear systems," *IEEE Trans. Control Syst. Technol.*, vol. 19, no. 6, pp. 1549–1558, Nov. 2010.
[37] Z. Hou and S. Jin, *Model Free Adaptive Control: Theory and Applications*. Boca Raton, FL, USA: CRC Press, 2019.
[38] X. Bu, Z. Hou, and H. Zhang, "Data-driven multiagent systems consensus tracking using model free adaptive control," *IEEE Trans. Neural Netw. Learn. Syst.*, vol. 29, no. 5, pp. 1514–1524, May 2018.
[39] H. Zhang, J. Zhou, Q. Sun, J. M. Guerrero, and D. Ma, "Data-driven control for interlinked AC/DC microgrids via model-free adaptive control and dual-droop control," *IEEE Trans. Smart Grid*, vol. 8, no. 2, pp. 557–571, Dec. 2015.
[40] D. Xu, Y. Shi, and Z. Ji, "Model-free adaptive discrete-time integral sliding-mode-constrained-control for autonomous 4WMV parking systems," *IEEE Trans. Ind. Electron.*, vol. 65, no. 1, pp. 834–843, Jan. 2017.
[41] D. Liu and G.-H. Yang, "Prescribed performance model-free adaptive integral sliding mode control for discrete-time nonlinear systems," *IEEE Trans. Neural Netw. Learn. Syst.*, vol. 30, no. 7, pp. 2222–2230, Jul. 2019.
[42] Z.-H. Pang, G.-P. Liu, D. Zhou, and D. Sun, "Data-based predictive control for networked nonlinear systems with network-induced delay and packet dropout," *IEEE Trans. Ind. Electron.*, vol. 63, no. 2, pp. 1249–1257, Feb. 2016.
[43] E. D. Sontag, "Input to state stability: Basic concepts and results," in *Nonlinear and Optimal Control Theory*. Cham, Switzerland: Springer, 2008, pp. 163–220.
[44] X. Su, X. Liu, and Y.-D. Song, "Event-triggered sliding-mode control for multi-area power systems," *IEEE Trans. Ind. Electron.*, vol. 64, no. 8, pp. 6732–6741, Aug. 2017.

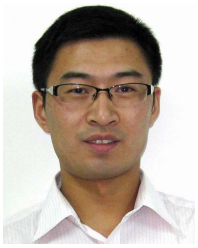

Xuhui Bu (Member, IEEE) received the B.S. and M.S. degrees in automation control from Henan Polytechnic University, Jiaozuo, China, in 2004 and 2007, respectively, and the Ph.D. degree in control theory and application from Beijing Jiaotong University, Beijing, China, in 2011.

He is currently a Full Professor with Henan Polytechnic University. He has authored over 60 peer-reviewed journal articles and over 20 papers in prestigious conference proceedings. His research interests include data-driven control, iterative learning control, traffic control, and networked system control.

Wei Yu (Student Member, IEEE) received the B.S. degree in rail transportation signal and control from Henan Polytechnic University, Jiaozuo, China, in 2018, where he is currently pursuing the M.S. degree in automation with the School of Electric Engineering and Automation.

His research interests include data-driven control and networked system control.

Yanling Yin received the B.S. and M.S. degrees from Henan Polytechnic University in 2004 and 2007, respectively.

She is currently a Lecturer at Henan Polytechnic University. Her research interests include learning control, integrated energy systems, and distributed optimization.

Zhongsheng Hou (Fellow, IEEE) received the B.S. and M.S. degrees in applied mathematics from the Jilin University of Technology, Jilin, China, in 1983 and 1988, respectively, and the Ph.D. degree in control theory and applications from Northeastern University, Shenyang, China, in 1994.

From 1997 to 2018, he was with Beijing Jiaotong University, Beijing, China, where he was a Distinguished Professor and the Head of the Department of Automatic Control. He is currently the Chair Professor with the School of Automation, Qingdao University, Qingdao, China. He has published over 200 journal articles. He has authored a monograph *Model Free Adaptive Control: Theory and Applications* (CRC Press, 2013). His research interests include data-driven control, model free adaptive control, learning control, and intelligent transportation systems.

Dr. Hou is the Founding Director of the Technical Committee on Data Driven Control, Learning and Optimization, Chinese Association of Automation (CAA). He is a fellow of CAA. He is an International Federation of Automatic Control (IFAC) Technical Committee Member of Adaptive and Learning Systems and Transportation Systems.